01 Jan 2022

Improving Age of Information with Interference Problem in Long-Range Wide Area Networks

Preti Kumari

Hari Prabhat Gupta

Tanima Dutta

Sajal K. Das
Missouri University of Science and Technology, sdas@mst.edu

Recommended Citation

P. Kumari et al., "Improving Age of Information with Interference Problem in Long-Range Wide Area Networks," *Proceedings - 2022 IEEE 23rd International Symposium on a World of Wireless, Mobile and Multimedia Networks, WoWMoM 2022*, pp. 137 - 146, Institute of Electrical and Electronics Engineers, Jan 2022.
The definitive version is available at https://doi.org/10.1109/WoWMoM54355.2022.00025

2022 IEEE 23rd International Symposium on a World of Wireless, Mobile and Multimedia Networks (WoWMoM) | 978-1-6654-0876-9/22/$31.00 ©2022 IEEE | DOI: 10.1109/WoWMoM54355.2022.00025

Improving Age of Information with Interference Problem in Long-Range Wide Area Networks

Preti Kumari[1], Hari Prabhat Gupta[1], Tanima Dutta[1], and Sajal K. Das[2]
[1]{pretikri.rs.cse17, hariprabhat.cse, tanima.cse}@iitbhu.ac.in, and [2]sdas@mst.edu
[1]Department of Computer Science and Engineering, IIT (BHU) Varanasi, India
[2]Department of Computer Science, Missouri University of Science and Technology, Rolla, USA

***Abstract*—Low Power Wide Area Networks (LPWAN) offer a promising wireless communications technology for Internet of Things (IoT) applications. Among various existing LPWAN technologies, Long-Range WAN (LoRaWAN) consumes minimal power and provides virtual channels for communication through spreading factors. However, LoRaWAN suffers from the interference problem among nodes connected to a gateway that uses the same spreading factor. Such interference increases data communication time, thus reducing data *freshness* and suitability of LoRaWAN for delay-sensitive applications. To minimize the interference problem, an optimal allocation of the spreading factor is requisite for determining the time duration of data transmission. This paper proposes a game-theoretic approach to estimate the time duration of using a spreading factor that ensures on-time data delivery with maximum network utilization. We incorporate the *Age of Information* (AoI) metric to capture the freshness of information as demanded by the applications. Our proposed approach is validated through simulation experiments, and its applicability is demonstrated for a crop protection system that ensures real-time monitoring and intrusion control of animals in an agricultural field. The simulation and prototype results demonstrate the impact of the number of nodes, AoI metric, and game-theoretic parameters on the performance of the IoT network.**

***Index Terms*—Age of information, game theory, IoT, long range communications.**

I. Introduction

The Internet of Things (IoT) is a fast growing paradigm whose sustainable growth and increased ubiquity depend on seamless integration with application environments. Various delay-sensitive applications (e.g., precision healthcare, smart agriculture, forest fire monitoring) require real-time update, low data rate, and minimal power consumption [1]. The Long-Range Wide Area Network (LoRaWAN) open specification is a Low Power WAN (LPWAN) protocol based on the Long-Range (LoRa) technology. An extensive coverage area and minimal energy consumption bring out the suitability of LoRa technology for smart IoT applications [2]–[4]. Building on top of the LoRa modulation scheme, as depicted in Fig. 1, the LoRaWAN comprises the end users (EUs), LoRa nodes (LNs), LoRa gateway (LG), network server (NS), and applications. The LNs acquire and transfer EUs' data to the LG using the LoRaWAN protocol.

The LoRa technology operates with Spreading Factors (SFs) ranging from 7 to 12, where SF7 provides the highest data rate with low sensitivity level at the receiver, whereas SF12 provides higher reception sensitivity at the cost of lower data rate [5]. Due to the high sensitivity level at the receiver end, the data transmitted using higher SFs is received at low dBm (decibel-milliwatt) that increases the eagerness of LNs to select the highest possible SF. The eagerness to select higher SF for data transmission is one of the principal causes for the *interference problem* in LoRa when multiple LNs are connected with a single LG [5], [6]. The interference leads to the increased delay of receiving the status update at the applications running on the NS. The mechanism of *rationally using* the allocated SF by an LN can reduce the interference problem. The LG pays price to the LNs for providing the data. To reduce the interference problem, the LG sets the price for using the SFs based on their load.

Fig. 1 illustrates an IoT application scenario, where the sensors acquire and transmit delay-sensitive information about the animals intruding an agriculture field, to the NS over the LoRa network. Ideally, the NS receives continuously fresh information about the physical phenomenon. However, it is often impractical to receive *fresh* information as the network adds some delay or packet loss due to the interference. To quantify such delay in the updates, we use the *Age of Information* (AoI) metric, defined as the time elapsed since the freshest packet was generated [7], [8]. In [9], the authors estimated the transmission time duration without considering the packets' AoI. The AoI increases with interference, which in turn decreases the network utility in terms of the received freshest packet. For example, the delay in the information updates from the agriculture field leads to severe deterioration of the crop yield. To mitigate the delay, there is a need to optimally utilize the available SFs for collecting up to date information that maximizes the network utility.

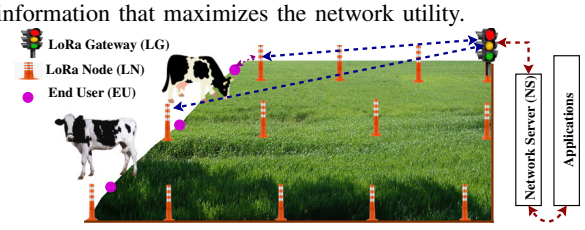

Fig. 1: A crop protection system using LoRa network.

This paper addresses an important problem: *How to reduce AoI in the LoRa network in presence of interference?* We propose a game-theoretic approach to determine the optimal time duration for data transmission on suitable SFs. Such optimal time helps reduce the interference among LNs during data transmission to the same LG. We use the AoI metric to maintain the freshness of data at the NS.

978-1-6654-0876-9/22/$31.00 ©2022 IEEE
DOI 10.1109/WoWMoM54355.2022.00025

A. Our Contributions

This paper makes the following major contributions.

• *Age of Information*: We quantify the freshness of data with the help of the AoI metric and derive an expression consisting of the queuing delay, communication delay, and service time.

• *Nash Equilibrium (NE) among LNs*: We formulate the interactions among LoRa nodes as a *Nash equilibrium game* for allocating the time duration of using the SFs.

• *Stackelberg Game (SG) between LG and LNs*: We formulate the interactions between LNs and LG as a *Stackelberg game* to reduce the effect of interference and improve network utility. At the follower (LN) and leader (LG) levels, we estimate the utility and formulate the optimization problems that estimate the optimal time allocated to each LN for using SFs. The goal is to satisfy the transmission time demand of each LN, requiring a minimum message delivery time in the network.

• *Performance:* We analyze the effectiveness of the proposed approach by simulating LoRa using Network Simulator-3. Experimental results demonstrate the impact of the number of LNs, AoI metric, and game-theoretic parameters on the performance of the IoT network.

• *Application:* We apply the proposed solution to CALR, a **C**rop protection system from **A**nimals using **L**ong **R**ange network. The system detects the animal intrusion, and communicates information to the application running on the network server (NS).

The rest of the paper is organized as follows. Section II introduces the preliminaries while Section III proposes a novel approach to estimating the time duration for data transmission from the LNs to the LG. Section IV presents experimental results. Section V is an application of the proposed approach to an agriculture field. Section VI concludes the paper.

II. Preliminaries

A. Network Topology

As shown in Fig. 2, LoRaWAN follows a star of star topology where multiple LNs can connect to multiple applications using the LG followed by an NS. The connection between the LNs and LG follows the LoRaWAN protocol, where each LN receives the data from the EUs and send them to the LG using the allocated SFs (ranging from SF7 to SF12). Fig. 2 also illustrates that LN_1 transmits data using the allocated SF7 and SF12, whereas LN_2 transmits data using SF7 and SF8. The LNs have to wait to get the allocated SFs free for data transmission. For example, SF7 is allocated first to LN_1 and then to LN_2, which has to wait until LN_1 completes its transmission on SF7. After receiving data from the LNs, the LG relays them to the NS for processing using non-LoRaWAN protocol. Further, the processed data are received on the applications running at the NS. While transmitting data from the LNs to the applications, the waiting and communication times are measured as the AoI, defined next.

B. Age of Information (AoI)

The Age of Information (AoI) quantifies the freshness of information [7], [8], [10]. Consider a source-destination pair,

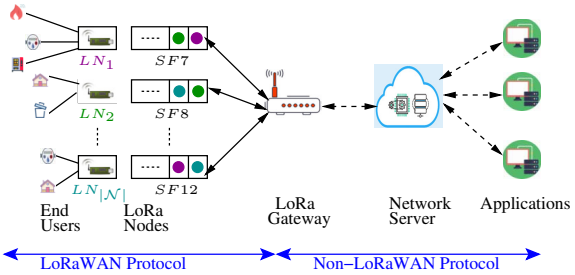

Fig. 2: Illustration of the LoRaWAN architecture.

where the source is the LN and destination is the NS. The source transmits the status update packets, generated by the EUs, to the destination. Then the AoI is the elapsed time since the last received status update that was generated. The goal of the delay-sensitive applications is to ensure that the status update packets reach on time. Let the ith packet with the generation time τ_i be received by the destination at time instance $\tau_i{}'$. Thus the age of packet i at $\tau_i{}'$ is equal to $(\tau_i{}'-\tau_i)$.

C. Stackelberg Game

The Stackelberg Game (SG) is a strategic interaction among the players on which some hierarchical competition takes place [11]–[14]. Here the LG and LNs are the players in the game, acting respectively as the leader and followers. The leader starts the game and selects a strategy (e.g., pricing strategy for using SFs). After observing the strategy of a leader, the followers respond by selecting their best strategies in response (e.g., the transmission time duration on the SFs). Then, the leader re-optimizes its strategy based on the best response strategies of the followers. The solution to the SG can be obtained by establishing a Stackelberg Equilibrium (SE) between the leader and followers, defined as follows.

Definition 1. *(Stackelberg equilibrium) Let* $\mathcal{N} = \{1, \cdots, n, \cdots, |\mathcal{N}|\}$ *be the followers set, where* $|\mathcal{N}|$ *is the total number of followers in the network. Let* $\mathbf{p}^{s*} = [p_1^{s*}, p_2^{s*}, \cdots, p_{|\mathcal{N}|}^{s}{}^{*}]$ *denote the strategy of the leader for all the followers, and* $\mathbf{t}^{s*} = [t_1^{s*}, t_2^{s*}, \cdots, t_{|\mathcal{N}|}^{s}{}^{*}]$ *be the vector of strategies of all the followers. Let* U^L *and* U_n^F *be respectively the utilities of a leader and a follower* $n \in \mathcal{N}$*. Then* $(\mathbf{p}^{s*}, \mathbf{t}^{s*})$ *is a Stackelberg Equilibrium (SE) if the following two conditions hold:*

$$U^L(\mathbf{p}^{s*}, \mathbf{t}^{s*}) \geq U^L(\mathbf{p}^{s}, \mathbf{t}^{s*}),$$
$$U_n^F(\mathbf{p}^{s*}, \mathbf{t}^{s*}) \geq U_n^F(\mathbf{p}^{s*}, \mathbf{t}^{s}), \forall n \in \mathcal{N}. \quad (1)$$

TABLE I: List of symbols

Symbol	Description	Symbol	Description
$\mathcal{N}$	Set of LNs	δ	Normalization parameter
n	Index of LNs	t_n^s	Time duration of nth LN
$\mathcal{S}$	Set of SFs	p_n^s	Price of nth LN
s	Index of SF	γ	Pricing coefficient
e_n^s	Price coefficient of end user	$\lambda_{n,1}, \lambda_{n,2}$	Lagrangian multipliers
α	Normalization parameter	a_n, b_n	Gain coefficient of LG

III. Estimating AoI and the Time Duration

This section proposes a novel Stackelberg Game (SG) approach to estimating the time duration of using the allocated spreading factors (SFs) by the LNs. This allocation maximizes

the network utility and minimizes interference. The proposed approach uses LNs (followers) that try to maximize utilities by increasing the transmission time and decreasing the energy consumption. On the other hand, the LG (leader) makes an optimal pricing strategy to maintain the freshness of data by estimating the AoI.

A. Estimation of AoI

The AoI in the network increases due to: (1) the queuing waiting time at the LN to free up the allocated SF, (2) the communication delay from the LN to the LG (and the LG to the NS), and (3) the service time.

Let the non-LoRaWAN network use a high-speed communication channel to transfer the data. It reduces the queuing waiting time and the communication delay at the LG and the NS to a smaller (almost negligible) value. Since there are six different virtual channels for SFs ranging from SF7 to SF12 to transmit the data, the age of status update from the LNs using two different SFs does not effect each other. Fig. 3 shows a sample variation of age $\Delta_n^s(\tau)$ for an arbitrary LN, say n, on an SF, say s, as a function of time (τ) at the NS. Let the initial age at $\tau = 0$ be $\Delta_n^s(0) = \Delta_0$. The time instances $\tau_{n,k}^s$ and $\tau'^s_{n,k}$ respectively indicate the generation time and reception time of the packet k from the LN n on the SF s. Let $X_{n,k}^s = \tau_{n,k}^s - \tau_{n,k-1}^s$ denote the inter-arrival time of the packets at the time instances $\tau_{n,k-1}^s$ and $\tau_{n,k}^s$. The system time $T_{n,k}^s = \tau'^s_{n,k} - \tau_{n,k}^s$ is the time difference between the generation and reception time instances of the packet k. Let Γ_n^s be the data generation rate from the EUs at the LN n for the SF s; and let μ is the service rate of the packet at the LG.

The AoI at the NS increases linearly with time in the absence of an updated packet. We divide the total AoI of the LN n for K packets on the SF s into two regions. Fig. 3 shows the evolution of the age of LN n for K packets using SF s. For clarity, we have removed the symbol s from the figure. The first region A_1 is accumulated by the consumed time starting from the first packet to the last packet of this source delivered using the SF s. The second region A_2 is the result of the received aged information in the sense that, on receiving a packet at the destination, the age is reduced and reset to a smaller value. For example, on receiving the second packet at the time instance $\tau'_{n,2}$, the age is reset to $\Delta(\tau'_{n,2}) = \tau'_{n,2} - \tau_{n,2}$ by subtracting the inter-arrival time $X_{n,2} = \tau_{n,2} - \tau_{n,1}$ from the accumulated age. The overall AoI received from the LN n on SF s is the colored area covered in A_1 and A_2 (see Fig. 3).

Lemma 1. *Let $\mathcal{G}_n^s$ and $\mathcal{G}_{-n}^s$ be respectively the generated load (arrival rate/service rate) on the SF s of LN n and all other LNs except LN n. Let $\hat{\mathcal{G}}_n^s = \mathcal{G}_n^s/(1-\mathcal{G}_{-n}^s)$ be the normalized load and C_n^s be the communication delay of LN n on SF s. Then the average age of LN n on SF s is given by*

$$\Delta_n^s = \frac{\beta_n^s(\hat{\mathcal{G}}_n^s, \mathcal{G}_{-n}^s)}{(1-\mathcal{G}_{-n}^s)\mu} + C_n^s, \tag{2}$$

where

$$\beta_n^s(\hat{\mathcal{G}}_n^s, \mathcal{G}_{-n}^s) = 1 + \frac{\Delta_0 - 2K}{\hat{\mathcal{G}}_n^s} + \frac{{\hat{\mathcal{G}}_n^s}^2}{1-\hat{\mathcal{G}}_n^s} + \mathcal{G}_{-n}^s {\hat{\mathcal{G}}_n^s}^2,$$

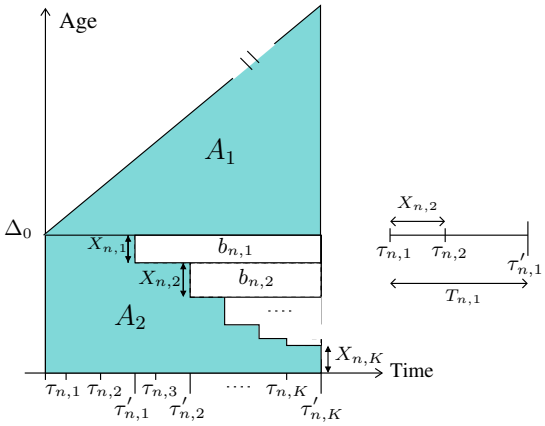

Fig. 3: Illustration of the evaluation of AoI of a LN n.

Proof. The average age over an interval $(0, \mathcal{T})$ is given by

$$\Delta_n^s = \frac{1}{\mathcal{T}} \int_0^{\mathcal{T}} \Delta_n^s(\tau) d\tau. \tag{3}$$

The area of region A_1 in Fig. 3, denoted by $\mathbf{A_1}$, is given by

$$\mathbf{A_1} = \frac{1}{2}\left[\left(\sum_{k=1}^{K} X_{n,k}^s\right) + T_{n,K}^s\right]^2. \tag{4}$$

The area of region A_2, denoted by $\mathbf{A_2}$, can be calculated by subtracting small rectangles from the biggest one as follows:

$$\mathbf{A_2} = \Delta_0\left[\left(\sum_{k=1}^{K} X_{n,k}^s\right) + T_{n,K}^s\right] - \sum_{k=1}^{K-1} b_{n,k}^s, \tag{5}$$

where $b_{n,k}^s = X_{n,k}^s\left[\left(\sum_{c=k+1}^{K} X_{n,c}^s\right) + T_{n,K}^s - T_{n,k}^s\right]$.

We observe that the age contribution, $T_{n,K}^s$, represents a finite boundary effect because it vanishes as K increases. Let the generation of data packets be represented as the arrivals of a stochastic process, and let $\Gamma_n^s = \lim_{\mathcal{T}\to\infty} \frac{K}{\mathcal{T}}$ be the rate of data generation from the EUs at LN n for SF s. Further, when the number (K) of generated packets becomes large, the sample average becomes the stochastic average. Applying Eqs. (4) and (5) to Eq. (3), we obtain

$$\begin{aligned}\Delta_n^s &= \frac{\Delta_0 \sum_{k=1}^{K} X_{n,k}^s + \sum_{k=1}^{K-1} X_{n,k}^s T_{n,k}^s - K\left(\sum_{k=1}^{K} X_{n,k}^s\right)^2}{\mathcal{T}}, \\ &= \Gamma_n^s\left(\Delta_0 E[X] + E[XT] - KE[X^2]\right),\end{aligned} \tag{6}$$

where E[.] is the expectation operator, and X and T are the random variables corresponding to the inter-arrival and system times, respectively. The SF is used by the LNs in a first-come-first-serve manner, i.e., the SF is allocated to those LNs first where the data arrived first. Other LNs with the same SF have to wait until the LN ahead in the queue is serviced. Let the data arrival and service processes follow Poisson and exponential distributions, respectively. The LN n uses M/M/1 queuing model with the arrival and service times as $\frac{1}{\Gamma_n^s}$ and $\frac{1}{\mu}$, respectively. Let C_n^s denote the communication delay from

the LN n to the LG on SF s which is equal to $\frac{(K*l)}{r_n^s}$ with the packet size l. Let d_n^s is the number of LNs in the network that uses the same SF as the LN n and creates interference. Then, by using Shannon's channel capacity formula [15], the transmission rate r_n^s between the LN n and the LG is defined as $W \log\left(1+\frac{\rho_n^s h_n^s}{\sum_{j=1}^{d_n^s}\rho_j h_j+\sigma^2}\right)$, where ρ_n^s, h_n^s, and σ^2 respectively denote the power used, the channel gain of LN n on SF s, and the power of additive white Gaussian noise. Since an SF can be allocated to multiple LNs [7], in the presence of multiple sources, Eq. (6) can be rewritten as

$$\Delta_n^s = \frac{\beta_n^s(\hat{\mathcal{G}}_n^s, \mathcal{G}_{-n}^s)}{(1-\mathcal{G}_{-n}^s)\mu} + C_n^s, \tag{7}$$

where $\beta_n^s(\hat{\mathcal{G}}_n^s, \mathcal{G}_{-n}^s) = 1 + \frac{\Delta_0 - 2K}{\hat{\mathcal{G}}_n^s} + \frac{\hat{\mathcal{G}_n^s}^2}{1-\mathcal{G}_n^s} + \mathcal{G}_{-n}^s \hat{\mathcal{G}_n^s}^2$. □

B. Estimating the Transmission Time Duration

In the crop protection system illustrated in Fig. 1, the owner of the field wants to be alerted on the intrusion of harmful animals. Suppose a network service provider deployed sensors (EUs) at the boundary of the crop field for sensing the presence of animals. They also installed LNs and LG for transmitting the collected sensory data to the NS. The applications running on the NS generate alerts that are received by the owner of the field. The owner needs to pay the LG via NS for using sensory data; thus the LG gains revenue (price) from the applications by providing data. Moreover, the LG pays a partial amount from the price gain to the LNs by forwarding the data. This is because the LNs consume their own resources for processing and forwarding data, and need to pay incentives to the EUs for energy consumption during data collection.

1) The Follower Level: In the LoRa system, the LNs gain price through the LG by providing data for applications running on the NS. The price depends on the freshness of the information received at the LG, which pays a high price for lower AoI; while it pays low price for higher AoI. Therefore, the price function can be defined as:

$$\mathcal{P}_n^s(\mathbf{t}) = \frac{p_n^s}{\Delta_n^s} - \gamma\left(\frac{\sum_{i\in\mathcal{N}} t_i^s}{\alpha}\right), \tag{8}$$

where γ is the pricing parameter that provides elasticity in pricing, α is a normalization parameter, p_n^s is the base price assigned by the LG to the LN n on SF s, and Δ_n^s is given in Eq. (7). As the age Δ_n^s of status update from the LN n on SF s increases, the LG's price gain decreases due to which the LNs select those SFs that maintain freshness of data. The price function also depends on the strategy of other LNs, namely $\mathbf{t} = [\mathbf{t}_1, \cdots, \mathbf{t}_n, \cdots, \mathbf{t}_{|\mathcal{N}|}]$, where $\mathbf{t}_n = [t_n^1, \cdots, t_n^s, \cdots, t_n^{|\mathcal{S}|}]$, modeled as the oligopoly market [13], in which the price is reduced when any LN transmits data for more time duration than the time duration estimated by the Stackelberg Equilibrium (SE). The LN $n \in \mathcal{N}$ needs to pay some cost to the EUs that generate the data, and also for consuming own energy for data transmission. Thus, the total utility of LN n is given by

$$\begin{aligned} U_n^F = &\text{ Price gained} - \text{End user cost} - \text{Energy consumption cost}, \\ =&\sum_{s=1}^{|\mathcal{S}|}\left[[\mathcal{P}_n^s(\mathbf{t})t_n^s] - \left(\frac{e_n^s t_n^s}{\delta} + \frac{e_n^s {t_n^s}^2}{\delta^2}\right) - \zeta\mathcal{E}_n^s t_n^s\right]. \end{aligned} \tag{9}$$

The first term indicates the price gain from the LG for transmitting the data for t_n^s time duration. The second term denotes the cost paid to the EUs by LN n. To formulate the EUs' cost, we apply the Taylor expansion on the logarithmic barrier function with pricing coefficient e_n^s due to its strict convexity. Finally, the third term represents the energy consumption cost with coefficient ζ to provide the same magnitude order as the price. In the competitive environment, each player aims at maximizing its utility and the follower level game can be formulated as follows.

$$\textbf{Follower Problem} \quad \max_{\mathbf{t}_n} \quad U_n^F(\mathbf{t}_n, \mathbf{t}_{-n}) \quad \text{such that } \sum_{s=1}^{|\mathcal{S}|} t_n^s \le t_n^{max}, t_n^s \ge 0,\ n \in \mathcal{N}, s \in \mathcal{S} \tag{10}$$

where $\mathbf{t}_n = [t_n^1, \cdots, t_n^s, \cdots, t_n^{|\mathcal{S}|}]$ is the vector of time duration of LN n for all SFs and $\mathbf{t}_{-n}$ is the vector of time duration of LNs except n for all SFs. The **Follower Problem** expresses that the LN n optimizes the strategy to maximize its utility; the constraint imposes that the data forwarding duration must not be higher than the duty cycle, t_n^{max}.

2) The Leader Level: In the LoRa network, the receiver sensitivity is low when the LNs forward the data using lower SF. Therefore, the LNs do not prefer data transmission voluntarily on lower SF, leading to load imbalance on the SFs. Such load imbalance increases the network delay, causing staleness of information. The leader (LG) solves this Follower Problem by making the pricing strategy such that the LNs are compelled to use lower SF for data forwarding and maximize the net utility. The leader's utility function is given by

$$\begin{aligned} U^L = &\text{ Generated revenue} - \text{Price paid to LNs}, \\ =&\sum_{n=1}^{|\mathcal{N}|}\sum_{s=1}^{|\mathcal{S}|}\left[a_n t_n^s - b_n(t_n^s)^2 - \mathcal{P}(\mathbf{t})t_n^s\right], \end{aligned} \tag{11}$$

where a_n and b_n are coefficients such that $a_n >> b_n$, which are used to measure the gain received from the data on the LG. The quadratic form of the utility function allows for tractable analysis and also serves as a good second-order approximation for the broader class of concave utility. In the Stackelberg game, the leader aims to maximize its revenue. The leader level game is formulated as follows.

$$\textbf{Leader Problem} \quad \max_{\mathbf{p}_n} \quad U^L(\mathbf{p}_n, \mathbf{p}_{-n}) \quad \text{such that} \quad p_n^s > 0, n \in \mathcal{N}, s \in \mathcal{S} \tag{12}$$

where $\mathbf{p}_n = [p_n^1, \cdots, p_n^s, \cdots, p_n^{|\mathcal{S}|}]$ is the vector of price of LN n for all SFs and $\mathbf{p}_{-n}$ is the vector of price of LNs except n for all SFs. The LG optimizes the strategy to maximize its

utility; and the constraint imposes that the price paid to the LN must be greater than or equal to zero.

3) Stackelberg Equilibrium of the Game: We use Eqs. (10) and (12) to derive the Stackelberg equilibrium of the game using backward induction method. The goal is to first determine the optimal strategy of a follower n (i.e., t_n^s), and then analyze the leader's strategy, x_n^s.

Theorem 1. *Let t_n^s be the strategy of the LN $n \in \mathcal{N}$ for data forwarding time duration on the SF $s \in \mathcal{S}$ to the LG. Then the best response $t_n^{s\star}$ of the LN n is given by*

$$t_n^{s\star} = \frac{1}{2\kappa_{2,n}^s}\left(Q_n^s - \frac{1}{\sum_{s=1}^{|\mathcal{S}|}\frac{1}{2\kappa_{2,n}^s}}\left(\sum_{s=1}^{|\mathcal{S}|}\frac{Q_n^s}{2\kappa_{2,n}^s} - t_n^{max}\right)\right),$$

$$\text{where } Q_n^s = \frac{p_n^s}{\Delta_n^s} - \kappa_{1,n}^s - \frac{\gamma}{\alpha}\sum_{j=1,j\neq n}^{|\mathcal{N}|} t_j^s - t_n^{max},$$

$$\kappa_{1,n}^s = \frac{e_n^s}{\delta} + \zeta\mathcal{E}_n^s + \frac{\gamma}{\alpha} \quad \text{and} \quad \kappa_{2,n}^s = \frac{\gamma}{\alpha} + \frac{e_n^s}{\delta}. \tag{13}$$

Proof. Using Lagrangian multipliers $\lambda_{n,1}$ and $\lambda_{n,2}$ for constraints defined in Eq. (10), we obtain

$$\mathcal{L}_n^F(\mathbf{t}_n, \mathbf{t}_{-n}) = \sum_{s=1}^{|\mathcal{S}|}\left[\left[\left(\frac{p_n^s}{\Delta_n^s} - \gamma\frac{\sum_{i\in\mathcal{N}} t_i^s}{\alpha}\right)t_n^s\right] - \left(\frac{e_n^s t_n^s}{\delta} - \frac{e_n^s {t_n^s}^2}{\delta^2}\right) - \zeta\mathcal{E}_n^s t_n^s\right] + \lambda_{n,1}t_n^s - \lambda_{n,2}\left(\sum_{s=1}^{|\mathcal{S}|} t_n^s - t_n^{max}\right) = 0,$$

$$\text{such that} \quad \lambda_{n,1}t_n^s = 0, \lambda_{n,2}\left(\sum_{s=1}^{|\mathcal{S}|} t_n^s - t_n^{max}\right) = 0,$$

$$\text{and} \quad \lambda_{n,1} \geq 0, t_n^s \geq 0, \lambda_{n,2} > 0. \tag{14}$$

Since the second derivative of $\frac{d^2\mathcal{L}_n^F(\mathbf{t}_n,\mathbf{t}_{-n})}{d(t_n^s)^2} = -2\left(\frac{\gamma}{\alpha} + \frac{e_n^s}{\delta}\right)$ is negative, the utility function in Expression (14) is concave and continuous. Hence the follower level game has at least one Nash Equilibrium (NE) [16]. The value of t_n^s can be obtained by setting the first derivative of the utility function to zero.

$$t_n^{s\star} = \frac{1}{2\kappa_{2,n}^s}\left(\frac{p_n^s}{\Delta_n^s} - \kappa_{1,n}^s + \lambda_{n,1} - \lambda_{n,2} - \frac{\gamma}{\alpha}\sum_{j=1,j\neq n}^{|\mathcal{N}|} t_j^s\right), \tag{15}$$

where $\kappa_{1,n}^s = \frac{e_n^s}{\delta} + \zeta\mathcal{E}_n^s + \frac{\gamma}{\alpha}$ and $\kappa_{2,n}^s = \frac{\gamma}{\alpha} + \frac{e_n^s}{\delta}$. From the constraint of Eq. (14), we obtain $\lambda_{n,1} = 0$; and by putting the value of t_n^s into the constraint of Eq. (14), we obtain

$$\lambda_{n,2} = \frac{1}{\sum_{s=1}^{|\mathcal{S}|}\frac{1}{2\kappa_{2,n}^s}}\sum_{s=1}^{|\mathcal{S}|}\frac{1}{2\kappa_{2,n}^s}\left(\frac{p_n^s}{\Delta_n^s} - \kappa_{1,n}^s - \frac{\gamma}{\alpha}\sum_{j=1,j\neq n}^{|\mathcal{N}|} t_j^s - t_n^{max}\right) \tag{16}$$

Substituting $\lambda_{n,2}$ from Eq. (16) into Eq. (15) completes the proof.

□

Next, we prove the following theorem.

Theorem 2. *The LG admits a unique optimal best response strategy given the optimal strategies of LNs.*

Proof. By using backward induction method from Eq. (13), the Lagrangian of the **Leader Problem** can be expressed as

$$\mathcal{L}^L(\mathbf{p}_n, \mathbf{t}_n) = \sum_{n=1}^{|\mathcal{N}|}\sum_{s=1}^{|\mathcal{S}|}\left(t_n^{s\star}\left(a_n - \frac{p_n^s}{\Delta_n^s} - \gamma\left(\frac{\sum_{i\in\mathcal{N}} t_i^s}{\alpha}\right)\right) - b_n(t_n^{s\star})^2\right) + \Lambda_1 p_n^s, \tag{17}$$

where Λ_1 is the Lagrangian multipliers of p_n^s.

To prove the uniqueness of the best response strategy of the LG, we use the Hessian matrix by taking the second order partial derivative of $\mathcal{L}^L(\mathbf{p}_n, \mathbf{t}_n)$ with respect to p_n^s and p_l^s:

$$\frac{d^2\mathcal{L}^L(\mathbf{p}_n,\mathbf{t}_n)}{dp_n^s dp_l^s} = \begin{cases}(\frac{\gamma}{\alpha}{t'_n}^s + \frac{1}{\Delta_n^s})(1 + {t'_n}^s) - 2({t'_n}^s)^2 b_n & \text{if } n = l,\\ 0 & \text{otherwise.}\end{cases} \tag{18}$$

where ${t'_n}^s = \frac{1}{2\kappa_{2,n}^s\Delta_n^s} - \frac{1}{2\kappa_{2,n}^s{\Delta_n^s}^2}\frac{1}{\sum_{s=1}^{|\mathcal{S}|}\frac{1}{2\kappa_{2,n}^s}}$. Since α is approximately equal to the forecast demand of data, its value is much larger than γ. The large value of α indicates that the first term is less than the second term in Eq. (18). Hence, the diagonal elements of the Hessian matrix provide negative values. The Hessian matrix of $\mathcal{L}^L(\mathbf{p}_n, \mathbf{t}_n)$ is strictly negative definite, which implies that the **Leader Problem** is a standard convex maximization problem. Hence the proof. □

The optimal solution of the **Leader Problem** can be obtained by applying Karush-Kuhn-Tucker conditions [17]. Therefore, the derivative of $\mathcal{L}^L(\mathbf{p}_n, \mathbf{t}_n)$ with respect to p_n^s is given as:

$$\frac{d\mathcal{L}^L(\mathbf{p}_n,\mathbf{t}_n)}{dp_n^s} = \left(a_n - \frac{p_n^s}{\Delta_n^s} - \gamma\left(\frac{\sum_{i\in\mathcal{N}} t_i^s}{\alpha}\right)\right){t'_n}^s\frac{t_n^s}{\Delta_n^s} + t_n^s{t'_n}^s\left(\frac{\gamma}{\alpha} - 2b_n\right) + \Lambda_1 = 0.$$

In Eq. (17), the Lagrangian variable should satisfy the expression $\Lambda_1 p_n^s = 0$. Since $p_n^s > 0$, Λ_1 must be equal to zero. The price of LN n for using SF s is estimated as

$$p_n^{s\star} = \Delta_n^s\left(a_n - \gamma\left(\frac{\sum_{i=1}^{|\mathcal{N}|} t_i^{s\star}}{\alpha}\right) + \frac{t_n^s}{{t'_n}^s\Delta_n^s} + t_n^s\left(\frac{\gamma}{\alpha} - 2b_n\right)\right),$$
$$\text{where } {t'_n}^s = \frac{1}{2\kappa_{2,n}^s\Delta_n^s} - \frac{1}{2\kappa_{2,n}^s{\Delta_n^s}^2\sum_{s=1}^{|\mathcal{S}|}\frac{1}{2\kappa_{2,n}^s}}. \tag{19}$$

The network holds an SE when the LG (leader) and the LNs (followers) respectively estimate the optimal price and time duration for data forwarding to maximize their utilities. We propose a Stackelberg Equilibrium algorithm (**SE Algorithm**) to find the equilibrium point using the best response strategy of LNs and optimal strategy of the LG. It estimates the time duration for using the allocated SFs by the LNs such that the network maximizes the utility and minimizes the interference. Step 7 of the **SE Algorithm** calculates the transmission time duration based on the selected price by the LG which maximizes the utility of the LNs. The LG re-optimizes the price based on the calculated transmission time duration as in Step 11 of the **SE Algorithm**. These steps are repeated till the utilities of the LG and LNs are maximized. A large number of nodes in the network increases the complexity of the algorithm which is expensive to run at the LNs due to its duty cycle and low processing capability. Therefore, the **SE Algorithm**

runs on the LG to compute the Stackelberg Equilibrium of the Game *i.e.,* optimal transmission time duration.

Algorithm 1: Stackelberg Equilibrium algorithm.

input : Terminating constants ω, ϵ, η $\tau_1 \leftarrow 0$,$\tau_2 \leftarrow 0$;
output: Optimal strategy $t_n^{s\star}$ of $n \in \mathcal{N}$ and $p_n^{s\star}$ of LG;

1 **do**
2 $\quad \tau_1 \leftarrow \tau_1 + 1$;
$\quad$ /* NE among followers: Each n maximizes its utility */
3 $\quad$ **do**
4 $\quad\quad Flag \leftarrow 0$;
5 $\quad\quad \tau_2 \leftarrow \tau_2 + 1$;
6 $\quad\quad$ **for** $n \leftarrow 1$ **to** $|\mathcal{N}|$ **do**
$\quad\quad\quad$ /*Using Eq. (13) for estimating $t_n^s[\tau_2+1]$. */
7 $\quad\quad\quad t_n^s[\tau_2+1] = \frac{1}{2\kappa_{2,n}^s}(Q_n^s[\tau_2] - \frac{1}{\sum_{s=1}^{|\mathcal{S}|}\frac{1}{2\kappa_{2,n}^s}}(\sum_{s=1}^{S}\frac{Q_n^s[\tau_2]}{2\kappa_{2,n}^s} - t_n^{max}))$;
8 $\quad\quad\quad$ **if** $(\|t_n^s[\tau_2+1] - t_n^s[\tau_2]\| > \eta)$ **then**
9 $\quad\quad\quad\quad Flag \leftarrow 1$;
10 $\quad$ **while** $(Flag == 1)$;
$\quad$ /* Stackelberg Equilibrium between the leader and follower: Use t_n^s and $p_n^s[\tau_1]$ for estimating $p_n^s[\tau_1+1]$ */
11 $\quad p_n^s[\tau_1+1] = p_n^s[\tau_1] + \epsilon \bigtriangledown_{U^L}(p_n^s[\tau_1])$;
12 **while** $(\|p_n^s[\tau_1+1] - p_n^s[\tau_1]\| < \omega p_n^s[\tau_1])$;

Example: Let us consider $|\mathcal{N}| = 3$ LNs connected to multiple end users in the LoRA network. Assume that $\mathbf{t}^{s0} = \{t_1^{s0}, t_2^{s0}, t_3^{s0}\}$ is the vector of initial transmission time duration of the three LNs. The Leader (LG) announces its initial pricing strategy for using SFs *i.e.,* $\mathbf{p}^{s0} = \{p_1^{s0}, p_2^{s0}, p_3^{s0}\}$. Based on $\mathbf{p}^{s0}$, the **SE Algorithm** calls Eq. (13) to calculate the followers' (LNs) best response strategies *i.e.,* the transmission time duration that leads to call Eqs. (7) for calculating the AoI of LNs for using SFs. The best response strategy is calculated for each LN and the utility of the followers is estimated as in Eq. (9) based on the new value of the transmission time duration, *i.e.,* $\mathbf{t}^{s1}$. This procedure continues till the utility of LNs increases based on the new calculated value of the transmission time duration and reaches the Nash equilibrium (NE). After calculating NE, the **SE Algorithm** calculates the new pricing strategy as given in Eq. (19) for using SFs *i.e.,* $\mathbf{p}^{s1} = \{p_1^{s1}, p_2^{s1}, p_3^{s1}\}$. If the utility of LG based on $\mathbf{p}^{s1}$ increases, then the procedure from step 2 - step 11 continues; else the SE Algorithm stops; and the last value of the transmission time duration and the price is the Stackerberg equilibrium, *i.e.,* $t_n^{s\star}$ and $p_n^{s\star}$.

4) Time Complexity of the SE Algorithm: Let q be the number of iterations at which the SE is calculated. To estimate the data transmission time duration, the LNs calculate the age of information (AoI) on each allocated SF to select the SF with low AoI. Assume that an LN uses $\mathbb{S}$ number of allocated SFs to calculate AoI, then Step 7 of the **SE Algorithm** runs for all $\mathbb{S}$ of the LN. Therefore, for all $|\mathcal{N}|$ number of LNs present in the network, the **SE Algorithm** requires $O(q|\mathcal{N}|\mathbb{S})$ time. As the maximum number of allocated SFs to the LNs is 6, the value of $\mathbb{S}$ is of constant time. As a result, the time complexity to find an SE in the LoRa network is $O(q|\mathcal{N}|)$.

IV. Performance Evaluation

This section evaluates the performance of the proposed approach through simulation experiments. Section IV-A describes the simulation setup while Section IV-B presents the impact of LNs on the network throughput and delay with and without considering the AoI metric. Section IV-C illustrates impact of the game parameters on the performance of the proposed approach. Specifically, we consider the pricing parameter and terminating constants η and ω. Section IV-D compares the performance of three existing works, such as random, distance, and equal interval based SF allocation. These baseline and widely used schemes [6], [18]–[20] for allocation of SFs motivate us to consider them for comparison.

A. Simulation Setup

We validate the performance of the proposed work by using Network Simulator-3 (NS-3) [21], [22]. The LoRaWAN MAC protocol in NS-3 supports multiple channels, SFs, LGs, and bi-directional networks with a large number of LNs. We repeated each experiment 100 times, and took the average. Simulation experiments consist of NS, LG and multiple LNs randomly deployed in a disc-shaped field with a radius of 2 kilometers similar to the outdoor experiments in [23]. From experiments we observe that 18 LNs exhibit efficient results for our proposed approach. Therefore, although the network has a lot of LNs, we consider only 18 LNs transmit their data at the same time by using an LG. The arrival of data from the EUs to the LN is modeled as M/M/1 queue and follows Poisson distribution. Most of the network parameters can be obtained from the datasheet of *LoRaWAN Multitech mDot* [24], [25]. The considered parameters in this paper are listed in Table II.

TABLE II: Parameter values used in the experiments.

Parameter	Symbol	Value
Signal bandwidth	W	125 kHz
Power consumption	ρ_n^s	$[2-14]$ dBm
Channel gain	h_n^s	0.2
Pricing coefficient of LG	γ	10
Pricing coefficient of EU	e_n^s	[0-1]
Gain coefficient	$\{a_n, b_n\}$	$\{100, 0.1\}$

B. Impact of the Number of LNs

This section illustrates the impact of the proposed approach on the network performance, without and with considering the AoI metric. The performance is measured in terms of network throughput and delay. The **SE Algorithm** calculates the transmission time duration with and without the AoI metric. We use three different deployment distributions of the LNs, such as uniform, Poisson, and random. In the uniform distribution, the LNs are deployed such that $\left(\frac{Number\ of\ LNs}{Number\ of\ SFs}\right)$ number of LNs come in the range of each SF. Whereas, in the Poisson distribution, the LNs are deployed by using $\frac{e^{-\Upsilon}\Upsilon^{\nu}}{\nu!}$, where ν is the number of times the spreading factor (SF) is allocated to the LN and Υ is the mean SF allocation. In the random distribution, the LNs are randomly deployed in the region.

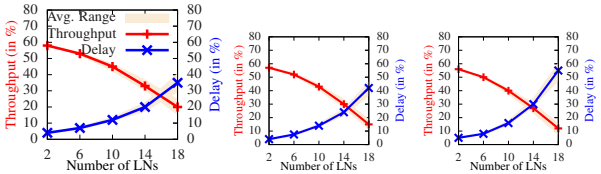

(a1)-(a3): Network performance without AoI metric for uniform, Poisson, random distribution, respectively.

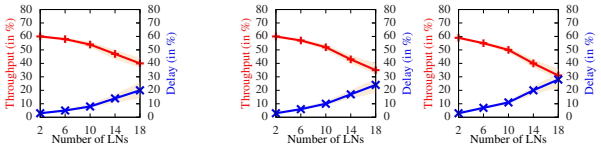

(b1)-(b3): Network performance with AoI metric for uniform, Poisson, random distribution, respectively.

Fig. 4: Impact of LNs on network throughput and delay.

Figs. 4(a1)–(a3) illustrate the network throughput and delay for uniform, Poisson, and random deployment distributions, respectively, without considering the AoI metric (i.e., removing Δ_n^s from Eq. 8) while making the pricing strategy. Whereas, Figs. 4(b1)–(b3) illustrate the network performance of the proposed approach considering the AoI metric. Experimental results demonstrate that the proposed approach with AoI increases throughput and decreases delay as compared to the approach without the AoI metric. This is because the LNs select those SFs which provide high price (set by the LG for low AoI) in our proposed approach, thereby decreasing the delay and increasing the throughput. An interesting observation is that the uniform distribution of LNs yields better result than the other two distributions. Therefore, the LG can be placed such that all LNs follow the uniform distribution with respect to the LG with a goal to maximize the network performance.

C. Convergence Rate and Impact of Game Parameters

This section studies the convergence rate of the **SE Algorithm** followed by the impact of game parameters on the utility of the network devices. Figs. 5(a1) and 5(b1) show the number of iterations after which the **SE Algorithm** converges for LNs and LG, respectively. Fig. 5(a1) shows the convergence result for 5 LNs $(LN_1, \cdots, LN_5)$. The convergence of the **SE Algorithm** for LG is also shown on different variations of gain ratio which is defined as the percentage of increment in the gain coefficient a_n and b_n of LG. The utility of LNs and LG for the proposed Stackelberg Game approach (SG), SF allocation with Random based (RB), Distance based (DB), and Equal-interval based (EB) schemes are compared in Figs. 5(a2) and 5(b2). In the Random based scheme, the allocation of SFs is done by uniform random choice, not depending on the location of the LNs, whereas the Distance based scheme allocates SFs to the LNs based on the strength of the received signal at the LG. In Equal-interval allocation schemes, the total network area is divided into 6 concentric circles, where each annulus gets an equal width. Fig. 5(a2) illustrates that the average utility of LNs decreases as the number of nodes connected to the LG increases, irrespective of the SF allocation scheme. The result shows that the average utility of LNs is higher when the SF allocation incorporates the proposed game model in comparison with the other schemes. Similarly, Fig. 5(b2) illustrates that the utility of LG initially increases rapidly along with increased number of LNs, but starts decreasing afterwards. This is due to the fact that the LG receives more data as the number of LNs increases, but beyond a threshold, the network faces the interference problem. We conducted simulation experiments to calculate the value of threshold as 15 LNs.

Next, we present the impact of the total number of LNs on the proposed game equilibrium. Fig. 5(a3) illustrates that as the number of LNs connected to the LG increases, the price set by the LG is distributed among more LNs, each of which gets less time for data transmission on the allocated SFs. Therefore, the utility of the LNs decreases when the number of the LNs increases and the value of γ decreases. Fig. 5(b3) shows the effect on the utility of LG as the number of LNs increases. Although the utility of LG initially increases, it starts decreasing after a threshold increment in LNs due to the interference similar to that in Fig. 5(a2).

Finally, we analyze the impact of the terminating constants (η and ω) on the convergence rate of the **SE Algorithm**, and the utility of LNs and LG. For high value of terminating constants, the **SE Algorithm** converges in a fewer iterations which reduce the time complexity but compromise on the optimal solution. However, for low value, the solution is more optimal, but it requires more time for convergence. Figs. 5(a4) and 5(b4) show the impact of η and ω on the rate of convergence. As η increases from 0.1 to 0.4, the required number of iterations decreases from 12 to 7. Similarly, the iterations required for convergence reduce from 8 to 6 when ω increases from 2 to 3. Figs. 5(a5) and 5(b5) illustrate that the average utility of LNs decreases while the utility of LG increases with the increase in the number of LNs. We observe from this result that the tuning of the pricing strategy and terminating constants can help balance the load on the SFs, thus reducing the interference problem, increasing the network utility, and reducing the time complexity of the solution.

D. Comparison with Existing Works

Let us now compare our proposed approach with existing works on the SF allocation schemes for improving network performance. The existing literature that analyzed the inter-SF interference and packet collision rate using different SF allocation schemes are based on random, distance, equal interval, equal area, and path-loss models [6], [18]–[20]. In Random based scheme, the SF allocation is done by uniform random choice whereas, distance based scheme allocates SF to the LNs based on the strength of the received signal at the LG. In equal interval and area allocation schemes, the total network area is divided into 6 concentric circles, where each annulus gets an equal width in the former scheme, while each annulus gets an equal area in the area allocation scheme. The path-loss allocation scheme defines annuli based on a path loss model. The authors in [19] compared the performance of equal-

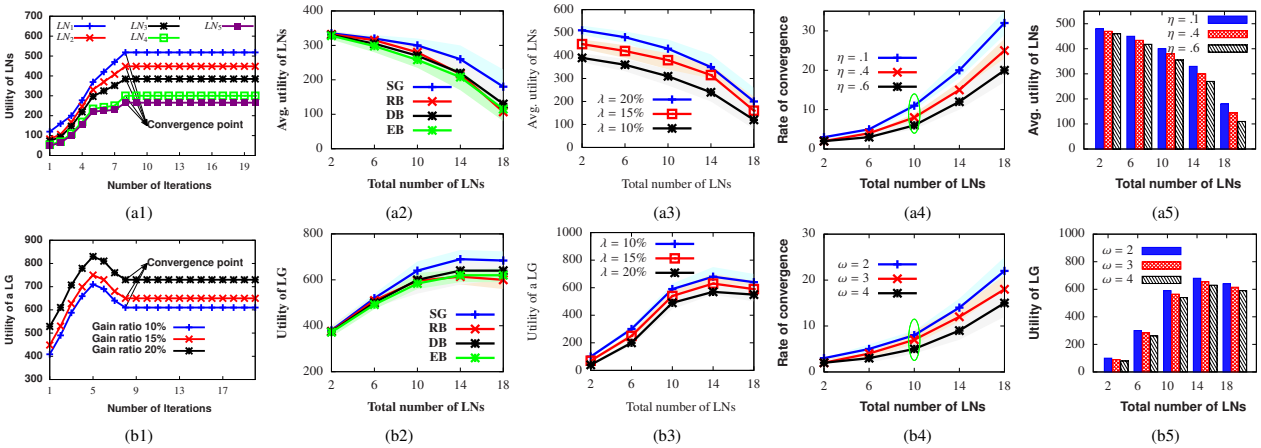

(a1) (a2) (a3) (a4) (a5)

(b1) (b2) (b3) (b4) (b5)

Fig. 5: Convergence rate of SE Algorithm and impact of the number of LNs on the utilities of LNs and LG and rate of convergence. Parts (a1)-(a5) and parts (b1)-(b5) show the results for LNs and LG, respectively.

interval, equal-area, and path loss model based SF allocation schemes; their results indicate that the equal-interval based allocation outperforms the equal-area, and path loss model based SF allocation schemes. Therefore, we consider equal-interval based allocation schemes for comparing with our proposed SG approach. Fig. 6 compares the proposed Stackelberg Game (SG) approach with random based (RB), distance based (DB), and equal-interval based (EB) SF allocation schemes. Similar to Fig. 4, we use uniform, Poisson, and random deployment distributions of LNs. Our proposed SF allocation scheme outperforms all other schemes for any number of LNs. This is because the proposed approach considers interactions among LNs and takes the allocation decision to maximize the utility of all LNs using game theory. Results demonstrate that the network performance is maximum and minimum for uniform and random distributions, respectively.

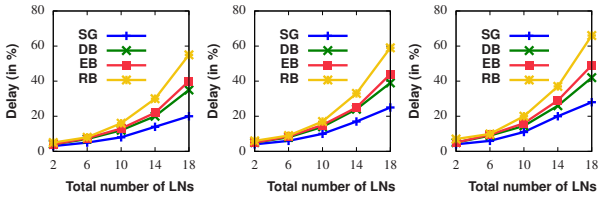

(a1)-(a3): Average delay of receiving packets for uniform, poisson, and random distribution, respectively.

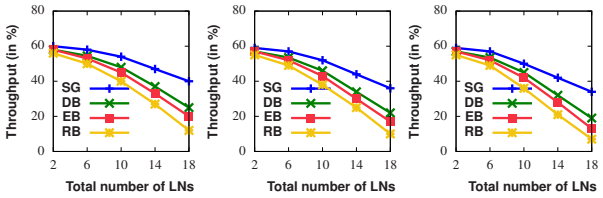

(b1)-(b3): Throughput of the network for uniform, poisson, and random distribution, respectively.

Fig. 6: Comparing proposed approach with existing work.

V. Application to an Agricultural Farm

This section demonstrates the application of the proposed approach to a system, called **C**rop protection system from **A**nimals using **L**ong **R**ange network (CALR) that we developed. The application estimates the time duration of using SFs by the LNs and detects sudden changes such as animals entering and roaming inside the agriculture farm. The CALR application is beneficial as it provides data transmission services without using multi-hop (short-range communication) or power-hungry communication (WiFi, 4G, or GPS) technology. We consider the deployment of sensors and LNs in the agricultural farm. The EUs (sensors) generate sensory data on the entry of local animals like buffaloes, cows, goats, etc.

A. Overview of CALR

The CALR uses sensors, LNs and LG. The animals entering the agriculture farm are detected by the EUs (sensors). Fig. 7(a) illustrates the configuration of CALR with the LNs, LG, and NS using LoRaWAN protocol to form a connected network. Passive infrared (PIR) motion detector sensors detect trespassing of animals by receiving the infrared radiation from the animal body when they are nearby the sensors. The resistance of the sensor varies inversely with the intensity of the infrared radiation. Therefore, with a sufficiently high infrared radiation, the resistance of the sensor drops to a low value and produces an electrical signal. The output of the sensor is connected to the analog-to-digital converter on the LN. Each LN is equipped with an ATmega328P Arduino Uno processing board, an SX1278 (Ra-02) LoRa module as shown in Fig. 7(b). The digital output after processing is referred as *sensory data*, which represents the distance between the sensors and the received radiation and lie in the range of 5 to 20m. We used Dragino LG01-S open source single channel Gateway as LG in the CALR. Numbers 1 - 7 in Fig. 7(b) indicate the prototype, deployment region, PIR motion detector sensor, LoRa module 868mhz, Arduino Uno, Dragino lora gateway, zooming of deployment region, respectively. At the NS, the cumulative sensory data from LGs are used to make the final decision.

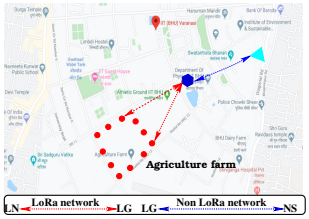

(a) CALR inside the campus.

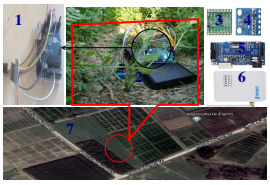

(b) Prototype devices.

Fig. 7: Illustration of CALR and experiments inside the campus of IIT (BHU), Varanasi, India. The LNs, LGs, and NS are indicated by the circle (●), hexagon (⬢), and triangle (◀), respectively.

B. Agriculture Farm Experiment

We deployed the CALR system in the agriculture farm inside the IIT (BHU) campus, as shown in Fig. 7(b). We deployed 16 LNs and one LG inside the farm, to ensure that the animals must be tracked and the network is connected with a high probability. To validate the animal tracking data collected by the network, we used a video camera to record the movement of animals, and the accuracy was computed by comparing the data from CALR and video camera. The accuracy (Acc) of CALR is defined as the ratio of the number of animal intrusions detected to the actual number of animal intrusions in the field. Let D denote the total number of animal intrusion data from the field. Then

$$Acc = \frac{1}{D}\sum_{i=1}^{D} \mathbf{1}\left(y_i == \bar{y}_i\right), \tag{20}$$

where y_i and $\bar{y}_i$ respectively denote the actual results of animal detection and results obtained from the CALR system to detect the animal intrusion. The function $\mathbf{1}(\cdot)$ is given as $\mathcal{F}$, where $\mathbf{1}(\mathcal{F})$ is equals to 1, if $\mathcal{F}$ is true; otherwise it is 0.

C. Experimental Results

1) Use Case: It is sometimes observed that the crop in the agricultural field is ravaged by animals which implies a huge financial loss for the farmers. In this experiment, we use the CALR to detect animals approaching near the field. Fig. 8 shows scenarios where the LNs are placed along the boundaries and inside the field. These LNs are associated with the LG for transferring data for a fixed time as estimated by the **SE Algorithm**. The LG further transferred the data to the NS, which accumulates the data for making a final decision. For example, a decision could be an alarm sound to woo the animals away from the field, or send messages to the farmers. This way the farmers will know about the ravage and arrive at the spot in case the animals do not turn away by the alarm.

Fig. 8(a1) shows the sensor intensity $\mathcal{I}_t = \{0, 10, 0\}$ at time t, indicating that an animal enters the field. It also shows that $\mathcal{I}'_t = \{0, 10, 0\}$ at time t', indicating that the animal is still inside the field. The difference of such time duration helps identify the duration of stay of the animal inside the field. Fig. 8(a2) shows that the sensor intensity at time t, $t+1$, $t+2$ are $\{0, 10, 0\}$ which indicates that a group of animals (e.g., a herd) entered the field. While the sensor continues to track the animals, the intensity of sensor value helps determine whether a big or small size animal entered the field. (The sensor intensity for bigger animal is very high compared to a smaller one.) Fig. 8(a3) shows that the intensity of sensors $\mathcal{I}$ and $\mathcal{I}'$ at time instance t are $\mathcal{I}_t = \{0, 5, 0\}$ and $\mathcal{I}'_t = \{0, 18, 0\}$, respectively, indicating that a big and a small size animals entered the field. Fig. 8(a) illustrates a scenario where the CALR system identifies the moving trajectory of a human inside the field. Let the location of three sensors $\mathcal{I}^1$, $\mathcal{I}^2$, and $\mathcal{I}^3$ be l_1, l_2, and l_3, respectively. The sensor intensities $\mathcal{I}^1_t = \{0, 18, 0\}$, $\mathcal{I}^2_{t'} = \{0, 18, 0\}$, and $\mathcal{I}^3_{t''} = \{0, 18, 0\}$ in Fig. 8(a4) indicate that the human moves from l_1 to l_3 via l_2.

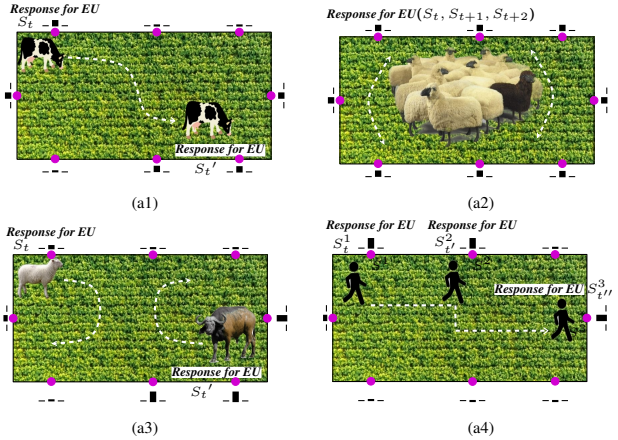

Fig. 8: Experimental scenarios of CALR, where an animal is detected by a sensor (EU) attached to the LN is indicated by (▬■▬) signal. The EUs are indicated by circle (●).

2) Accuracy of CALR: Since we monitored the agriculture field with a video camera, we could verify the events of animals entering and human detected by CALR. The results corresponding to the entry of animal, herd, human, stay duration of the animal inside the field, and moving trajectory detection experiments are presented in Table III. We conducted a total of ten experiments, each of 120 minutes. Table III shows the results when the CALR experiments use the proposed Stackelberg game (SG), random based (RB), distance based (DB), and equal-interval based (EB) SF allocation schemes for forwarding data from the LG to NS. The overall accuracy of CALR when using the proposed SG for detecting the entry of animal, herd, human, stay duration of animal inside the field, and moving trajectory are above 95%, 96%, 92%, 91%, and 93%, respectively. The results show that the proposed work provides higher accuracy as compared to other existing schemes. This improvement is due to the fact that the RB and DB schemes suffer from the high packet drop. Therefore, the NS is incapable of making a correct decision. On the oher hand, the EB scheme does not fully utilize the SF. We also observed that the CALR using SG detects animals or human which are in the proximity range of the sensor, whereas the video recording captures images unnecessarily of those animals or human which are sufficiently far from the sensor.

TABLE III: Results of the CALR system using Camera recording (CR), proposed Stackelberg game (SG), random based (RB), distance based (DB), and equal-interval based (EB).

Exp.No.:	1	2	3	4	5	6	7	8	9	10	**Total**	**Accuracy(%)**
Part (a): Entry of the animal												
CR:	20	17	18	19	17	18	18	20	19	18	184	
SG:	18	15	18	18	15	18	18	19	19	16	**174**	174/184=94.57%
RB:	17	15	16	18	14	18	16	17	19	16	**166**	166/184=90.22%
DB:	17	15	16	18	14	16	15	15	18	14	**158**	158/184=85.87%
EB:	17	15	16	16	13	14	15	15	16	12	**149**	149/184=80.98%
Part (b): Entry of herd												
CR:	15	16	13	16	17	13	14	11	14	11	**140**	
SG:	14	16	12	16	17	12	14	10	13	11	**135**	135/140=96.43%
RB:	13	15	10	14	16	10	11	9	12	11	**121**	121=140=86.43%
DB:	13	14	10	13	13	10	12	10	11	10	**116**	116/140=82.86%
EB:	12	13	11	11	14	12	11	9	12	10	**115**	115/140=82.14%
Part (c): Entry of human												
CR:	10	9	12	13	14	14	12	12	9	10	115	
SG:	10	7	11	11	13	13	11	12	8	10	**106**	106/115=92.17%
RB:	9	7	9	11	12	11	11	11	8	10	**99**	99/115=86.09%
DB:	10	6	9	10	13	13	11	11	8	10	**101**	101/115=87.83%
EB:	10	6	10	10	13	11	10	12	8	10	**100**	100/115=86.96%
Part (d): Stay duration of animal inside the field												
CR:	14	13	12	15	14	13	13	14	15	15	138	
SG:	12	11	11	13	13	12	13	13	13	15	**126**	126/138=91.30%
RB:	12	10	9	11	13	11	12	13	12	15	**118**	118/138=85.51%
DB:	11	10	9	13	13	10	13	13	12	14	**118**	118/138=85.51%
EB:	11	10	10	11	11	11	12	13	12	14	**115**	115/138=83.33%
Part (e): Moving trajectory detection												
CR:	10	9	11	13	12	11	10	10	11	12	109	
SG:	9	7	10	11	11	10	10	10	11	12	**101**	101/109=92.66%
RB:	9	6	9	10	11	10	9	9	11	11	**95**	95/109=87.16%
DB:	8	7	8	11	10	8	9	10	11	12	**94**	94/109=86.24%
EB:	9	7	10	11	10	9	9	8	11	12	**96**	96/109=88.07%

VI. Conclusion

In this paper, we proposed a Stackelberg Game (SG) approach for optimizing the use of allocated SF to the LNs with the help of the age of information (AoI) metric. The proposed SG approach estimates the optimal time allocated to each LN for using SFs. It satisfies the transmission time demand of each LN and requires a minimum delivery time of messages in the network. The Nash equilibrium is established among the connected LNs at which all devices choose their optimal transmission time duration. The network reaches at a Stackelberg equilibrium when an LG (leader) estimates the optimal price for maximizing its utility. Experimental results demonstrate that the AoI metric improves the network performance in terms of delivery ratio, throughput, delay, and utility of devices. We believe that this work would motivate further research in the area of optimal SF allocation in the LoRa system for improving the network performance.

Our analysis did not consider the fault-tolerant LoRa network in which some devices (LN and LG) may be down due to low battery power or hardware failure. Future directions of research include faulty devices to make a fault-tolerant LoRa network to guarantee data delivery. Alongside, secure data communication is an essential future direction to explore.

References

[1] B. Akesson, M. Nasri, G. Nelissen, S. Altmeyer, and R. I. Davis, "An Empirical Survey-based Study into Industry Practice in Real-time Systems," in *2020 IEEE Real-Time Systems Symposium (RTSS)*, 2020, pp. 3–11.

[2] K. Abdelfadeel, T. Farrell, D. McDonald, and D. Pesch, "How to Make Firmware Updates over LoRaWAN Possible," in *2020 IEEE 21st International Symposium on "A World of Wireless, Mobile and Multimedia Networks" (WoWMoM)*, 2020, pp. 16–25.

[3] G. Premsankar, B. Ghaddar, M. Slabicki, and M. D. Francesco, "Optimal Configuration of LoRa Networks in Smart Cities," *IEEE Transactions on Industrial Informatics*, vol. 16, no. 12, pp. 7243–7254, 2020.

[4] J. Ortín, M. Cesana, and A. Redondi, "Augmenting LoRaWAN Performance With Listen Before Talk," *IEEE Transactions on Wireless Communications*, vol. 18, no. 6, pp. 3113–3128, 2019.

[5] N. El Rachkidy, A. Guitton, and M. Kaneko, "Collision Resolution Protocol for Delay and Energy Efficient LoRa Networks," *IEEE Transactions on Green Communications and Networking*, vol. 3, no. 2, pp. 535–551, 2019.

[6] A. Waret, M. Kaneko, A. Guitton, and N. El Rachkidy, "LoRa Throughput Analysis With Imperfect Spreading Factor Orthogonality," *IEEE Wireless Communications Letters*, vol. 8, no. 2, pp. 408–411, 2019.

[7] R. D. Yates and S. Kaul, "Real-time status updating: Multiple sources," in *Proc. ISIT*, 2012, pp. 2666–2670.

[8] B. Buyukates, A. Soysal, and S. Ulukus, "Age of Information Scaling in Large Networks," in *Proc. ICC*, 2019, pp. 1–6.

[9] P. Kumari, H. P. Gupta, and T. Dutta, "A Nodes Scheduling Approach for Effective Use of Gateway in Dense LoRa Networks," in *IEEE International Conference on Communications (ICC)*, 2020, pp. 1–6.

[10] S. Kaul, R. Yates, and M. Gruteser, "Real-time status: How often should one update?" in *Proceedings IEEE INFOCOM*, 2012, pp. 2731–2735.

[11] P. Kumari, H. P. Gupta, and T. Dutta, "A Stackelberg Game based River Water Pollution Monitoring System using LoRa Technology," in *16th Annual IEEE International Conference on Sensing, Communication, and Networking (SECON)*, 2019, pp. 1–5.

[12] G. E. Rahi, S. R. Etesami, W. Saad, N. B. Mandayam, and H. V. Poor, "Managing Price Uncertainty in Prosumer-CentricEnergy Trading: A Prospect Theoretic Stackelberg Game Approach," *IEEE Transactions on Smart Grid*, vol. 10, no. 1, pp. 702–713, 2019.

[13] M. J. Osborne *et al.*, *An introduction to game theory*. Oxford university press New York, 2004.

[14] T. D. Tran, L. B. Le, T. T. Vu, and D. T. Ngo, "Stackelberg Game-Based Network Slicing for Joint Wireless Access and Backhaul Resource Allocation," in *Proc. ICC*, 2019, pp. 1–7.

[15] T. M. Cover and J. A. Thomas, *Elements of Information Theory*. Wiley-Interscience, 2006.

[16] L. Shi, L. Zhao, G. Zheng, Z. Han, and Y. Ye, "Incentive Design for Cache-Enabled D2D Underlaid Cellular Networks Using Stackelberg Game," *IEEE Transactions on Vehicular Technology*, vol. 68, no. 1, pp. 765–779, 2019.

[17] M. Li, "Generalized Lagrange Multiplier Method and KKT Conditions With an Application to Distributed Optimization," *IEEE Transactions on Circuits and Systems*, vol. 66, no. 2, pp. 252–256, 2019.

[18] L. Amichi, M. Kaneko, E. H. Fukuda, N. El Rachkidy, and A. Guitton, "Joint Allocation Strategies of Power and Spreading Factors with Imperfect Orthogonality in LoRa Networks," *IEEE Transactions on Communications*, pp. 1–1, 2020.

[19] A. Mahmood, E. Sisinni, L. Guntupalli, R. Rondón, S. A. Hassan, and M. Gidlund, "Scalability Analysis of a LoRa Network Under Imperfect Orthogonality," *IEEE Transactions on Industrial Informatics*, vol. 15, no. 3, pp. 1425–1436, 2019.

[20] J. Lim and Y. Han, "Spreading Factor Allocation for Massive Connectivity in LoRa Systems," *IEEE Communications Letters*, vol. 22, no. 4, pp. 800–803, 2018.

[21] R. Brecht, Q. Wang, and S. Pollin, "A LoRaWAN Module for Ns-3: Implementation and Evaluation," in *Proc. WNS3*, 2018, pp. 61–68.

[22] F. V. den Abeele, J. Haxhibeqiri, I. Moerman, and J. Hoebeke, "Scalability Analysis of Large-Scale LoRaWAN Networks in ns-3," *IEEE Internet of Things Journal*, vol. 4, no. 6, pp. 2186–2198, 2017.

[23] N. Vatcharatiansakul, P. Tuwanut, and C. Pornavalai, "Experimental performance evaluation of LoRaWAN: A case study in Bangkok," in *2017 14th International Joint Conference on Computer Science and Software Engineering (JCSSE)*, 2017, pp. 1–4.

[24] "Lorawan multitech mdot," 2019. [Online]. Available: https://www.semtech.com/uploads/documents/SX1272_DS_V4.pdf

[25] L. Casals, B. Mir, R. Vidal, and C. Gomez, "Modeling the Energy Performance of LoRaWAN," *Sensors*, vol. 17, no. 10, pp. 1–30, 2017.